Available online at www.sciencedirect.com
SCIENCE DIRECT
ELSEVIER
Tectonophysics 409 (2005) 73–84
TECTONOPHYSICS
www.elsevier.com/locate/tecto

Geoelectric investigation of the Hellenic subduction zone using long period magnetotelluric data

D. Galanopoulos [a], V. Sakkas [b], D. Kosmatos [b], E. Lagios [b,*]

[a] General Secretariat for Civil Protection, Ministry of Interior, 2 Evangelistrias Str, 10563 Athens, Greece
[b] Department of Geophysics and Geothermics, University of Athens, Panepistimiopolis-Ilissia, 15784 Athens, Greece

Received 21 February 2005; received in revised form 1 July 2005; accepted 7 August 2005
Available online 6 October 2005

Abstract

The strongest evidence up to date for a subduction zone in the Hellenic region is a clearly identified Wadati-Benioff zone below the central Aegean Sea, to a maximum depth of 180 km. Alternative seismic tomography models suggest that subduction process continues deeper than the Wadati-Benioff zone to a maximum depth of at least 600 km. So far the lack of deep electrical studies in the region impeded scientists from imposing other control factors than seismic to the proposed models for the Hellenic Subduction Zone (HSZ). A Long Period Magnetotelluric (LMT) study was carried out in the southern part of the Greek mainland to study the deep electrical characteristics of the HSZ and examine whether prominent modelled features correlate with structures identified by the seismic methods. The study comprised collection, processing and modelling of magnetotelluric (MT) data in the period range 100–10000 s from ten sites located along a 250 km NE–SW trending profile. The dimensionality of the data was examined at a pre-modelling stage and it was found that they do not exhibit three-dimensional (3-D) features. The latter enabled to construct both one-dimensional (1-D) and two-dimensional (2-D) models. The proposed geoelectric model for HSZ was based on 2-D modelling, since it had better maximum depth resolution of about 400 km, and revealed structures not detected by 1-D modelling attempts. The model structure which was related to the African and Euro-Asian lithosphere is relatively resistive (>800 Ω-m) and has an average thickness of 150–170 km. Although the bottom of the lithosphere is adequately resolved, the Wadati-Benioff zone that delineates the top of the subducting lithospheric slab is not identified by any electrical feature. The modelled structure associated with the subducting part of the African lithosphere penetrates a relatively conductive (<200 Ω-m) asthenosphere with a dip angle of 42°. Intermediate electrical resistivities (200–800 Ω-m) are attributed to the ascending melting part of the lithosphere below the region of the Hellenic Volcanic Arc (HVA) and to a dipping zone below the south-western part of the profile, at 170–220 km depths.

Keywords: Long period magnetotellurics; Geoelectric; Hellenic subduction zone; Hellenic volcanic arc

1. Introduction

The subduction of the African Plate under the Eurasian one is the dominant tectonic process (McKenzie, 1978; Le Pichon and Angelier, 1979; Angelier et al., 1982) to account for the intense seismicity and the past or present volcanism (Fytikas et al., 1984) of the Hellenic region. The first strong evidence for a subducting lithospheric slab was an identified Wadati-Benioff zone below the central Aegean Sea to a maximum depth of 180 km (Galanopoulos, 1963; Papazachos, 1973). The seismicity zone was later confirmed with additional and

* Corresponding author.
E-mail addresses: galanopoulos@gscp.gr (D. Galanopoulos), vsakkas@geol.uoa.gr (V. Sakkas), lagios@geol.uoa.gr (E. Lagios).

0040-1951/$ - see front matter © 2005 Elsevier B.V. All rights reserved.
doi:10.1016/j.tecto.2005.08.010

more accurate seismological data, which included the Hellenic mainland (Makropoulos and Burton, 1984; Papadopoulos et al., 1986; Papazachos et al., 2000). The dipping angle of the subducting slab below the Central Aegean Sea was determined to be 30–40° (Papazachos, 1973). Further studies implied that the slab may be separated into two branches, a shallow one (20 km$\leq h \leq$100 km) with a dip angle of about 30°, and a deeper one (100 km$\leq h \leq$180 km) with a dip angle of about 45° (Hatzfeld et al., 1989; Papazachos et al., 2000).

Regarding the maximum penetration depth and the dip angle of the subducting slab, the above model is compatible with the ideas that subduction zones are primarily controlled by the polarity of their direction, i.e. W-directed or E- to NNE-directed, which is probably due to the westward drift of the lithosphere relative to the asthenosphere. Recalling observations in the Pacific Ocean, W-directed subduction zones (e.g. Marianas) are steep (up to 90°) and deep (down to 670 km) with respect to those directed to the East (e.g. Chile), which are on average shallower and less inclined. The Pacific asymmetry is also present in the Central Mediterranean where the Apennines and the Hellenic subduction zones are NW- and NE-directed zones, respectively, which seem to obey this rule (Doglioni et al., 1999). Alternatively, the suggestion that the subducting lithospheric slab penetrates deeper than the Wadati-Benioff zone to a maximum depth of at least 600 km (Ligdas et al., 1990; Ligdas and Main, 1991; Spakman et al., 1988, 1993) is compatible with some ideas on subduction zone seismicity associated with the thermal and rheological properties of subducting slabs (Wortel, 1982; Hobbs and Ord, 1988).

The average thickness of the Eurasian lithosphere in the Hellenic region is estimated to be between 90 and 120 km (Papazachos, 1969; Payo, 1967, 1969; Calganile et al., 1982). Undoubtedly our most up-to-date knowledge for the dipping angle and the maximum penetration depth of the subducting lithospheric slab and the thickness of the Eurasian lithosphere is principally based on the results of the already referenced seismic studies and the results of the gravimetric studies (Chailas et al., 1993; Lagios et al., 1995; Papazachos, 1994; Tsokas and Hansen, 1997). Although a series of broadband (10^{-2}–10^{+4} s) MT studies (Hutton et al., 1989; Galanopoulos et al., 1991,1998 Dawes and Lagios, 1991; Tzanis and Lagios, 1993, 1994; Lagios and Galanopoulos, 1998; Lagios et al., 1998; Sotiropoulos et al., 1996) were undertaken along the HVA, the layout of the MT sites did not allow determination of the deep electrical structure beyond the region of the arc.

The main objectives of this paper are therefore first to construct an electrical model for HSZ along the present NE–SW trending profile across the southern part of the Hellenic mainland (Fig. 1), and secondly to examine whether prominent features of this model correlate with structures identified by the earlier seismic methods.

2. The LMT data analysis

The present study involves LMT measurements in the period range 10^{+2}–10^{+4} s. The data were collected at ten stations located along a 250 km profile having a NE–SW direction across the southern part of Greece (Fig. 1: Profile AA′). The identification of the LMT sites together with their co-ordinates is given in Table 1. The main components of each LMT station were a geologger system and a telluric pre-amplifier box designed and built by the National Environment Research Council (UK), a three-component EDA magnetometer, and a set of non-polarising Pb–$PbCl_2$ electrodes, which were set up in the field 100 m apart having an L-shaped configuration.

Due to the bad data quality of sites 8 and 9, the data analysis concerned only the LMT sites 0–7. The results of data processing and analysis included period variations of apparent resistivity and phase values and in the measured directions, as it is illustrated for the LMT site 2 in Fig. 2a and b. The method suggested by Groom et al. (1993) was applied to address the dimensionality of the data. Following the methodology described in this paper, the fit of the data to a 1-D parameterisation, to a $5N$ free parameter 2-D model (i.e. period-dependent strike), to a $4N+1$ degrees of freedom 2-D model (i.e. period-independent strike), and finally to a $7N$ free parameter 2-D model (i.e. period-dependent regional strike) was successively tested. The logarithm of the parameter γ^2 was adopted as a misfit criterion to provide a quantitative measure of the fit of the data to these models. A parameterisation model is acceptable for further interpretation when 95% of the values of the above misfit criterion are less than 4. For the 1-D parameterisation, the rotationally invariant quantity $Z_{\mathrm{inv}}=(Z_{xx}Z_{yy}-Z_{xy}Z_{yx})^{1/2}$ was used, while for the definition of the strike angle in the case of the $5N$ free parameter 2-D model, the Swift angle was calculated. The Groom and Bailey (1989) tensor decomposition (GB tensor decomposition) was performed in the case of the $7N$ free parameter 2-D model.

Fig. 3a and b show the period variation of the log γ^2 misfit criterion for sites 1 and 3. The illustrated patterns are representative for the majority of the MT sites. Both

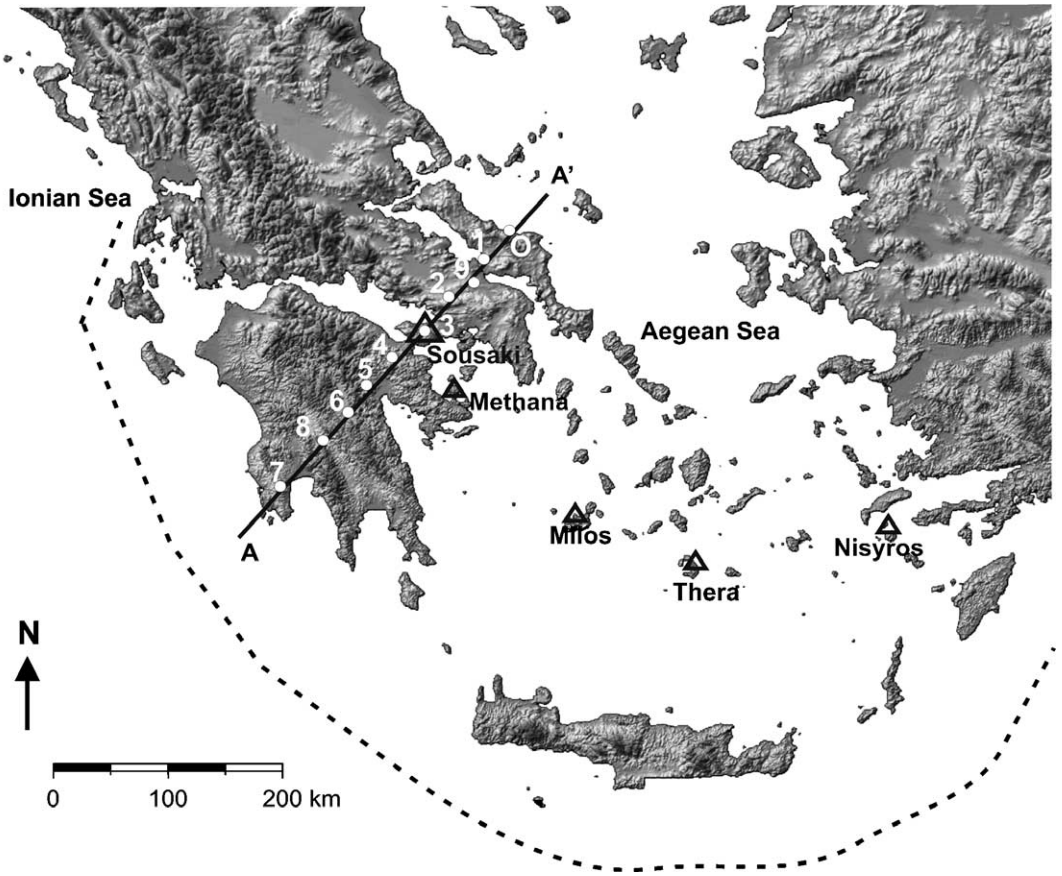

Fig. 1. Geographic location of the LMT profile AA′. Solid circles: LMT sites; solid line: LMT profile; dashed line: the Hellenic Trench; open triangles: volcanic centers along the Hellenic Volcanic Arc.

the 1-D and 2-D parameterisations are characterised by low misfit values. In the case of 1-D model and both the 5*N* and 4*N*+1 parameter 2-D models (Swift tensor decomposition), 100% of the misfit values are less than 2. In the case of the 7*N* parameter 2-D model (GB tensor decomposition), 100% of the misfit values are less than zero. According to Groom et al. (1993) low misfit values could be attributed to small data uncertainties. This is not however the case for the present MT data, since the uncertainties in the apparent resistivity and phase values are more than 15% and 25%, respectively.

Fig. 4a and b illustrate the period variation of Swift angle corresponding to the 5*N* free parameter 2-D model for sites 1 and 3. The same figures include the period variation of the GB regional strike for direct comparison. The illustrated patterns are representative for the majority of MT sites. Swift angle seems to be nearly period-independent and about N50°W, while this is not valid for the GB regional strike. According to Jones and Groom (1993), the GB regional strike is usually the least stable parameter when telluric distortion occurs. In order to stabilize the estimates of strike, the twist and shear have to be constrained. This task was not carried out, because the 5*N* parameterisation provides an acceptable fit and a nearly period-independent Swift angle of about N50°W, which corresponds well with the strike of the HSZ at the point of intersection with the MT profile. Thus, it was decided to adopt this angle as the main regional electrical strike for the 2-D modelling and interpretation.

3. The LMT data modelling

Since 1-D parameterisation provides an acceptable fit to the MT data (Fig. 3a and b), prior to the 2-D modelling, an attempt was made to model the data by using the "Most Squares" 1-D modelling algorithm introduced by Meju and Hutton (1992). The rotationally invariant quantity $Z_{\mathrm{inv}}=(Z_{xx}Z_{yy}-Z_{xy}Z_{yx})^{1/2}$ for

Table 1
LMT site names and coordinates

Site number	Area/site name	Geographic coordinates	
		Latitude (°)	Longitude (°)
0	Amfithea	38.61	23.76
1	Artaki	38.52	23.64
2	Inoi	38.17	23.41
3	Soussaki	37.96	23.14
4	Spathovouni	37.85	22.80
5	Kaparelli	37.67	22.51
6	Thanas	37.48	22.37
7	Rizomilos	37.10	21.90
8	Dafni	38.36	22.28
9	Inofita	38.35	23.55

the modelling of the LMT data from sites 1, 2, 3 and 4, as well as the impedance tensor elements relating the N–S and E–W measuring directions for the modelling of the data from sites 5 and 6, were used, respectively.

Table 2 provides for each 1-D model of each LMT site the calculated and expected χ^2 misfit values giving a measure of the fit of the 1-D model responses to the observed data. The expected χ^2 misfit was considered to be equal to $2N$, where N is the number of modelled periods. Table 2 shows that the condition of one dimensionality, i.e. calculated $\chi^2 < 2N$, is satisfied by the data of all the LMT sites.

The 1-D models derived for each LMT site were collated along the NE–SW profile AA′ (Fig. 1), and are presented for discussion in Fig. 5. This section does not include models for sites 0 and 7 since at the stage of 1-D modelling the data from these sites were not yet available.

The adopted geoelectric model for HSZ was finally based on the results of the 2-D modelling. In the presence of 2-D electric structures, the MT apparent resistivity and phase data may split into two independent modes that are called transverse electric (TE) and transverse magnetic (TM), respectively. The TE mode involves electric current flow parallel to strike, while the TM mode involves electric current flow perpendicular to strike.

The LMT data were modelled two-dimensionally along the Profile AA′ (Fig. 1) by using a computer program developed by Mackie (1996) and based on

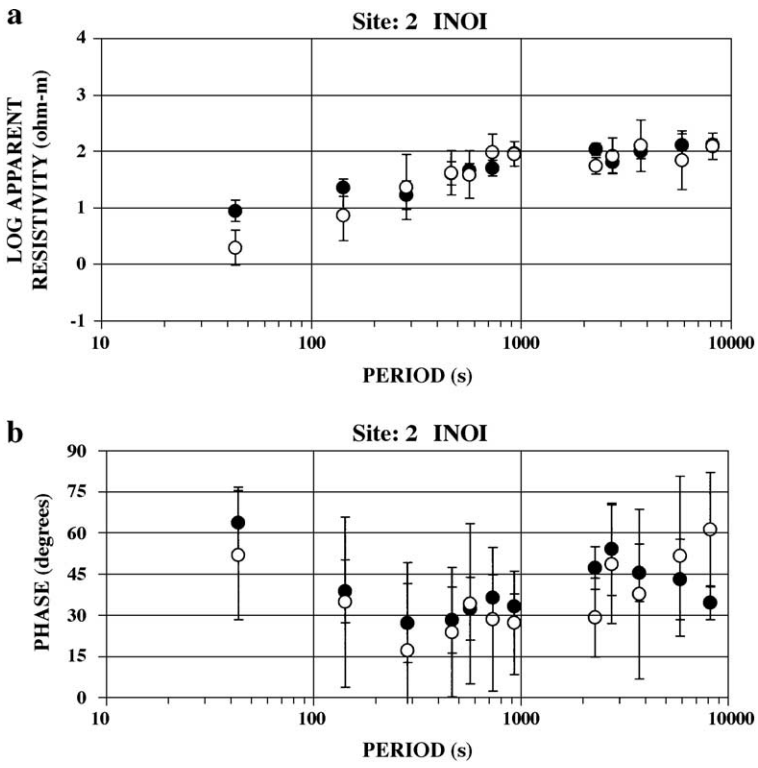

Fig. 2. The LMT data for site 2. (a) Period variation of apparent resistivity values in the measured directions. (b) Period variation of phase values in the measured directions. Solid circles: north–south direction; open circles: east–west direction.

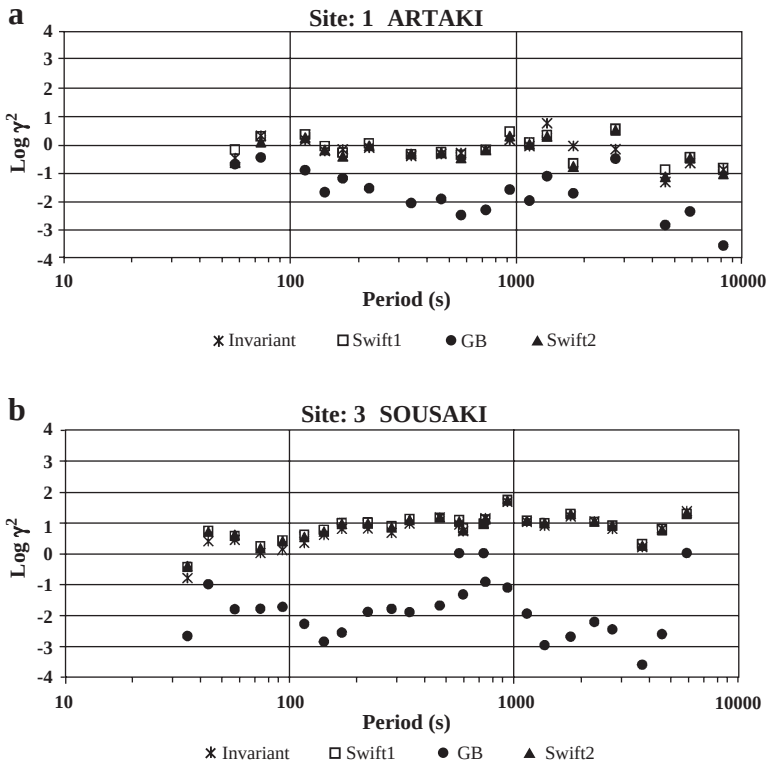

Fig. 3. Period variations of the log γ^2 misfit criterion for: (a) LMT site 1. (b) LMT site 3. Stars: 1-D model; open squares: 5N free parameter 2-D model; solid circles: 4N+1 parameter 2-D model; solid triangles: 7N free parameter 2-D model.

the method introduced by Mackie et al. (1988). The program requires a starting model and various input parameters. The used starting model was based on independent geological data and the results of the 1-D modelling. The region to be modelled was divided by a number of horizontal and vertical lines into a mesh of rectangular cells of variable sizes. The intersections of the horizontal and vertical lines form the nodes of the grid. There were three factors that have been considered in determining the grid spacing (Madden and Mackie, 1989). First, the spacing had to adequately describe the important electrical parameter of the area of interest. Secondly, the errors in the approximation resulting from the discretization had to be at an acceptable level. Thirdly, limits had to be imposed on the computational effort involved in obtaining the solution. Additionally, all the rules for a proper grid design described by Wannamaker et al. (1986, 1987) have been applied for the final model discretization. Following the above rules the finally adopted grid size was 75×75 elements. The grid was extended down to 450 km depth, excluding the last 4 rows that were used as the basal half space. The grid was more detailed between the depth interval of 40 to 300 km. Special care was taken to add more grid elements in areas of certain interest (e.g. close to station 3—Fig. 1). The topography was not included in the model, since it does not significantly change along the profile.

The input parameters apart from the observed TE and TM apparent resistivity and phase data included a noise floor for these data, the expected *rms* misfit, and a smoothing factor that controls the trade-off between fitting the data and adhering to the model constraint. The observed TE and TM mode apparent resistivity and phase data were obtained by rotating the measured electrical impedance tensor elements to the main regional electrical strike (50° W). The TE and TM mode data were modelled with equal weighting and a 5% noise floor. According to Mackie (1996) the smoothing factor should optimally be chosen so that the *rms* misfit for the inversion is between 1.0 and 1.5. Few inversion runs were performed to determine the best value for the smoothing factor. A factor of 5 was finally decided upon and used during the whole modelling procedure.

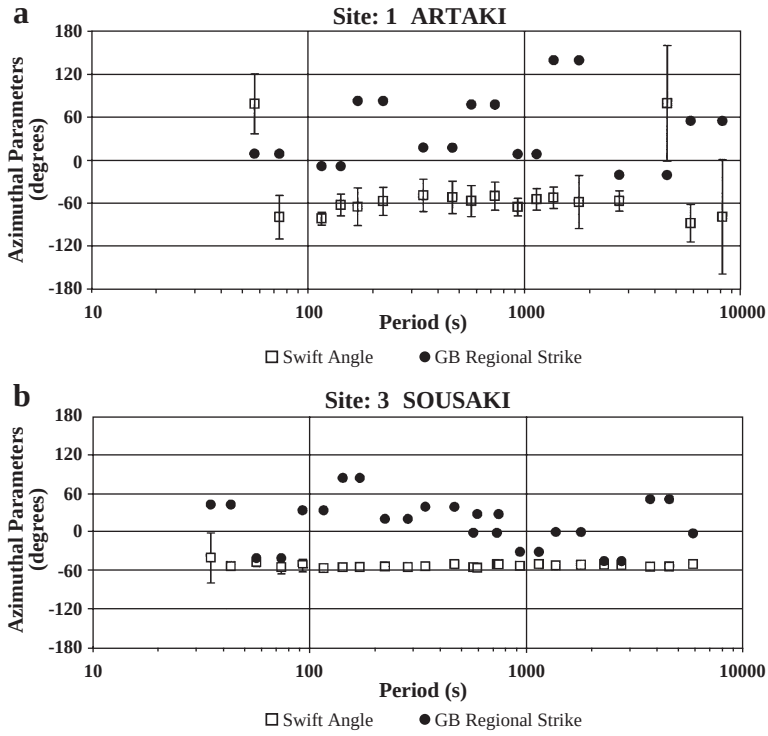

Fig. 4. Period variations of the GB regional strike (solid circles) and Swift angle corresponding to the 5*N* free parameter 2-D model (open squares) for: (a) LMT site 1. (b) LMT site 3.

Following the logistics of most MT inversion algorithms, Mackie's computer program minimises the misfit between the model and observed TE and TM resistivity and phase data over a number of iterations by keeping fixed the block geometry of the initial model and varying only the model resistivities. The model misfit in this paper is provided in both qualitative and quantitative manner. The qualitative way comprises comparison of contour sections of the model and observed resistivity and phase responses, while the quantitative way involves calculation of *rms* values.

The 2-D modelling comprised inversion of both TE and TM mode data. A total number of 386 data values were used. The best-fit model was obtained after 32 iterations and had an *rms* value of 0.22. The 2-D model is shown for discussion in Fig. 6, while the observed and model TE and TM resistivity and phase responses are shown in Figs. 7 and 8. The observed and calculated resistivity responses for both the TE and TM modes correlate reasonably well. Due to the fact that phase data are always more sensitive to noise, the correlation between the observed and calculated phase responses is not so prominent, it is however better for the case of TM mode.

4. Tectonic implications of electrical models

Fig. 5 shows the collated "Most Squares" 1-D layered models superimposed on a contour section based on the Niblett–Bostick transformation (Jones, 1983). The "Most Squares" models illustrate a maximum depth resolution of about 370 km, while the Niblett–Bostick model is limited to 350 km. The two layers of 30–170 Ω-m and 170–520 Ω-m, overlying a relatively more conductive (10–25 Ω-m) halfspace distinguish the electrical structure derived by the "Most Squares" models. A fairly similar electrical structure is observed along the HVA, below Milos (central part) and Nisyros (eastern part) islands (Galanopoulos, 1993). The main electrical feature of both the Niblett–Bostick and "Most Squares" sections is a relatively conductive region (<250 Ω-m) observed below the central part of the profile (sites 2, 3 and 4). This region extends to a maximum depth of about 250 km and is bounded laterally by two less conductive (>450 Ω-m) blocks, which extend to depths that approach the maximum depth resolution of the Niblett–Bostick model. Below the NE part of the profile, the first layer has a constant thickness of

Table 2
The fit of the 1-D model responses to the observed data by using the χ^2 misfit criterion

Site number	Area/site name	χ^2 misfit values	
		Calculated	Expected
1	Artaki	13.1	36
2	Inoi	7.3	24
3	Soussaki	1.1	50
4	Spathovouni	4.7	32
5	Kaparelli	6.1	32
6	Thanas	2.3	38

about 30 km. Below the SW part of the profile the thickness of the same layer varies from 25 to 45 km. The second layer has a variable thickness of about 100–320 km. The lower interface of this layer shows a large depression below sites 6, 5 and 4, while below sites 3, 2 and 1 it dips towards the NE at an angle of about 42°.

Below the south-western half of the profile, the electrical discontinuity between the first two layers of the Most Squares models is located at Moho depths resolved by the seismic studies of Makris (1985), Ansorge et al. (1992), and Van der Meijde et al. (2003). This correlation is better below the LMT site 6, where the electric and Moho discontinuities are determined at depths of 45 and 43 km (Van der Meijde et al., 2003), respectively.

The second layer of the Most Squares models could probably be associated with the deeper part of the lithosphere. The lower interface of this layer varies from 150 to 370 km, with an average depth of about 250 km below the centre of the profile. This average depth is comparable with the 220 km seismic discontinuity located under continents and island arc regions known as Lechmann discontinuity (Gu et al., 2001; Deuss and Woodhouse, 2002). According to Gu et al. (2001), Lechmann discontinuity is a local feature frequently associated with a rheological boundary separating a rigid continental plate from a more plastic convecting mantle below. The relatively conductive region (<250 Ω-m) below the central part of the profile, which includes the HVA (Site 3 in Fig. 5), could be related to a less rigid, probably melted part of the lithosphere.

The 2-D model of Fig. 6 suggests a rather simple geoelectric structure for HSZ. The model with respect to the observed vertical resistivity contrasts can be divided into three zones: A relatively conductive (<200 Ω-m) lower zone (170–400 km), a less conductive (>200 Ω-m) intermediate zone (40–270 km), and an electrically unresolved upper zone (0–40 km).

The upper zone (Zone A in Fig. 6) according to its relative depth range seems to correspond to the Earth's crust, but due to the lack of short period MT data it has a poorly resolved electrical structure, blanked for this reason in Fig. 8. The intermediate zone (Zone B in Fig.

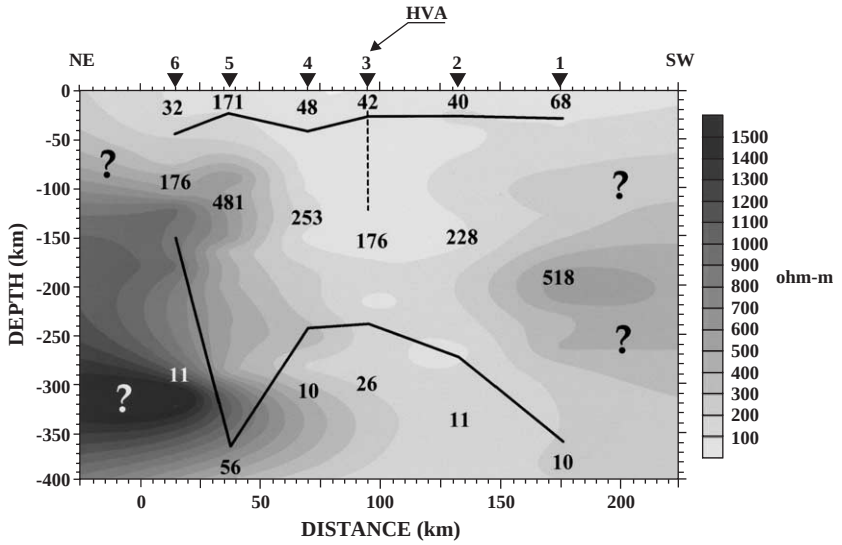

Fig. 5. The collated "Most Squares" 1-D models superimposed on a contour section based on the Niblett–Bostick transformation. Solid lines and figures: "Most Squares" layer boundaries and resistivities in Ω-m; scale bar: Niblett–Bostick resistivity range; question marks: poorly resolved structures.

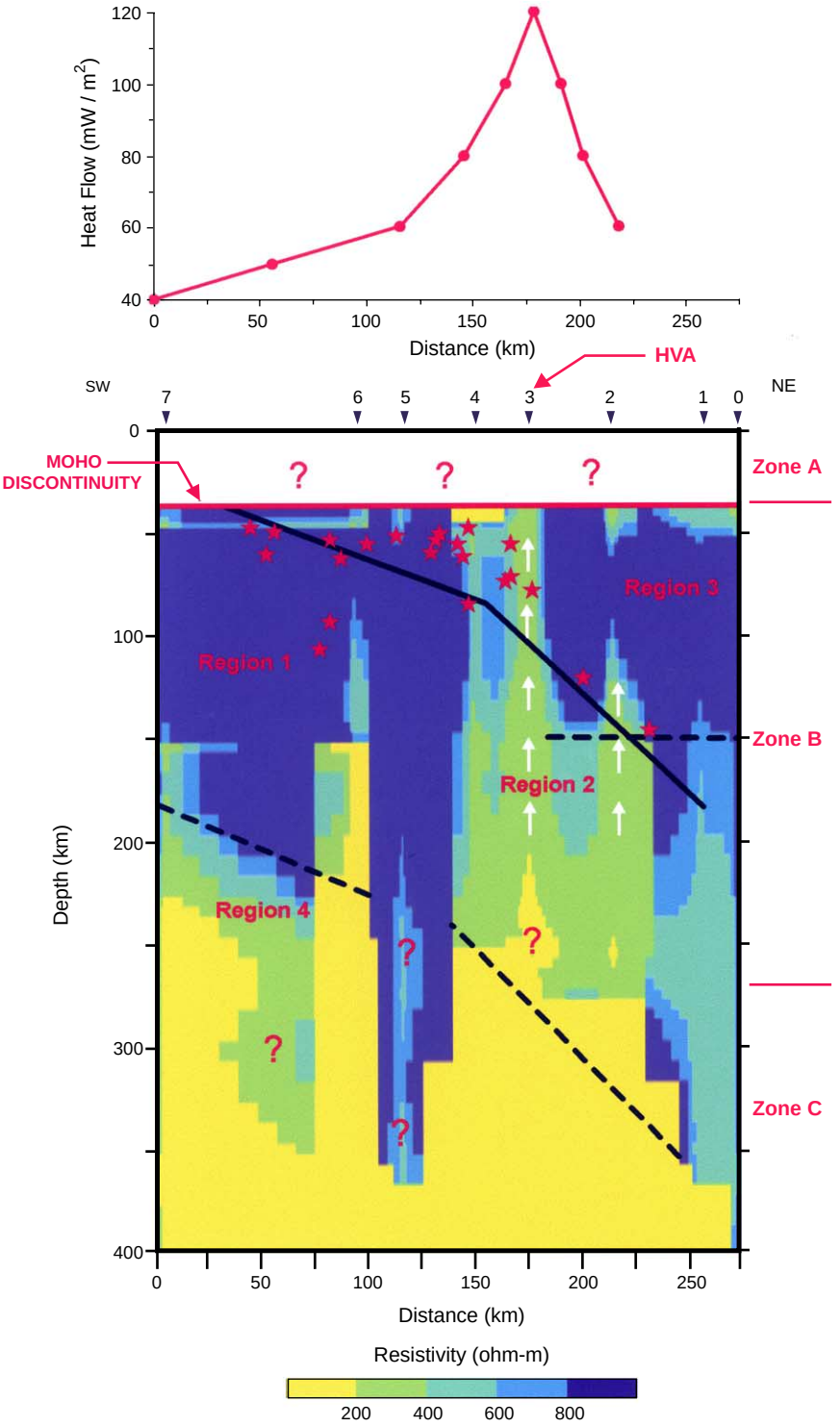

Fig. 6. The 2-D model together with seismic and heat flow data. Red solid stars: earthquake loci by Hatzfeld et al. (1989); black solid lines: Wadati-Benioff zone by Papazachos et al. (2000); dashed lines: inferred electrical boundaries; white arrows: probable magma flow; question marks: poorly resolved structures.

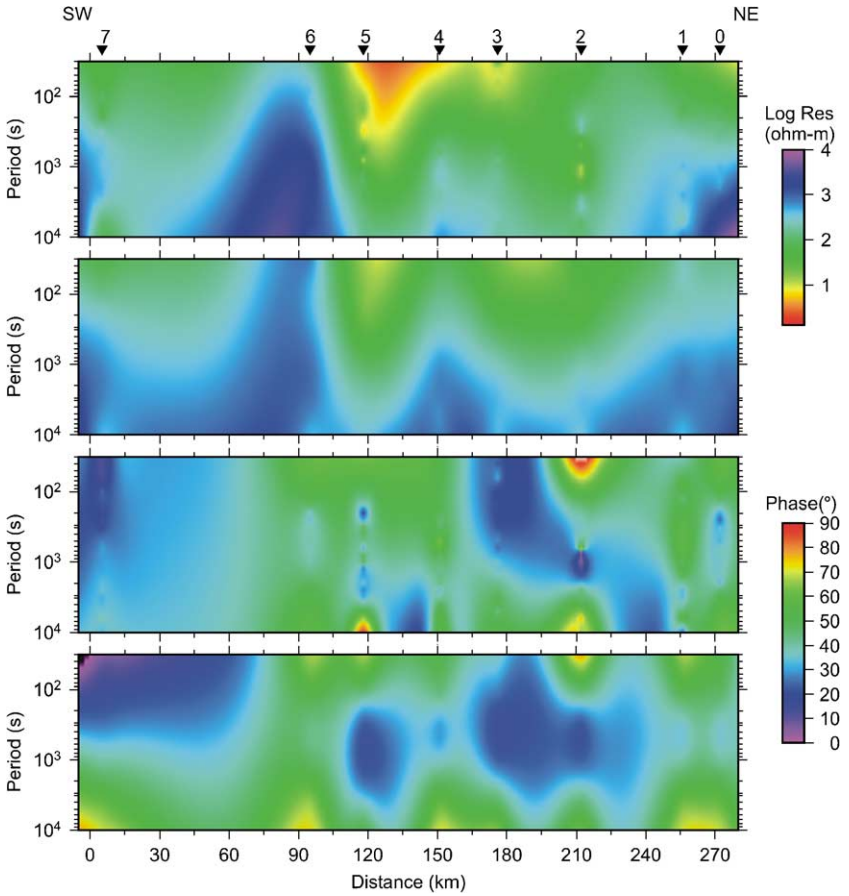

Fig. 7. The fit of the 2-D model responses to the observed data for the case of TE mode. From top to bottom: observed resistivity-model resistivity-observed phase-model phase.

6) according to the observed lateral resistivity contrasts is divided into three distinct regions, annotated by 1, 2 and 3, respectively.

The first region (Region 1 in Fig. 6) is located below sites 7, 6 and 5, and is relatively resistive (>800 Ω-m). This region could be related to the unmelted and thus rigid part of the subducting African lithosphere. The second region (Region 2 in Fig. 6) is situated below sites 4, 3 and 2 and has intermediate electrical resistivities (200–800 Ω-m). The main features of this region are two thin vertical zones having resistivities 200–400 Ω-m. The first zone is located below sites 4 and 3 (Soussaki Volcanic Centre) with a depth range of 40–200 km, while the second zone is located below site 2 in a depth range of 120–170 km. Although the electrical resistivity of these thin zones is quite high to be directly related to hot magma, since they are correlated (Fig. 6) with an observed relatively high heat flow anomaly, 125 mW/m^2 (Fytikas and Kolios, 1979), Region 2 could be associated with a less rigid, probably melting or partially melting part of the subducting African lithosphere. Regarding the first zone, which could be related to HVA, a possible explanation for this discrepancy would be the fact that Soussaki is not classified among the active volcanic centres of HVA, such as Thera (Santorini) and Nisyros (Fytikas et al., 1984). Alternatively the discrepancy could be attributed to the actual limitations of the resolving power of the MT method in the case of "small targets" at quite large depths. In such a case the expected low resistivity (10–20 Ω-m) of hot magma is masked by the higher resistivity of the surrounding lithosphere. Additionally, the second zone could be associated with the deep electrical structure of a second inner volcanic arc described by Fytikas et al. (1984).

The third region (Region 3 in Fig. 6) is located below sites 1 and 0; it has similar resistivities (>800 Ω-m) with the Region 1 and should correspond to the rigid material of the Euro-Asian lithosphere.

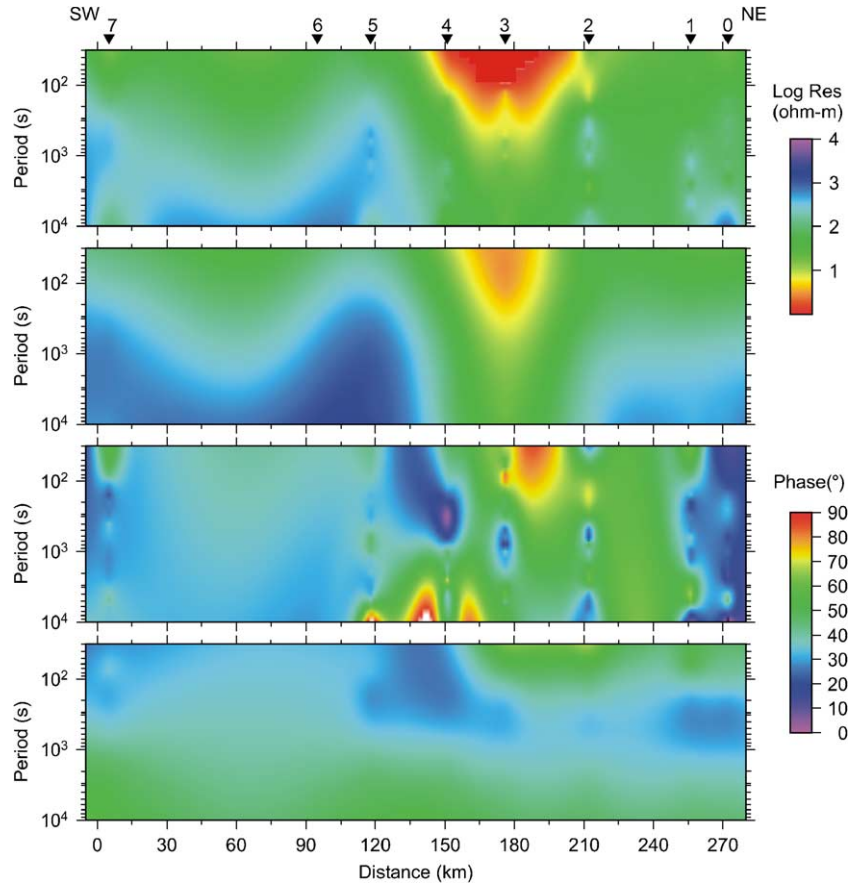

Fig. 8. The fit of the 2-D model responses to the observed data for the case of TM mode. From top to bottom: observed resistivity-model resistivity-observed phase-model phase.

The lower interface of the intermediate zone B dips from SW to NE with an average angle of 42°. This angle is compatible with the dip angle of 45° observed by Hatzfeld et al. (1989) and Papazachos et al. (2000) for the deeper branch (100 km≤h≤180 km) of the Wadati-Benioff zone. The average penetration depth of this zone is about 250 km.

The lower zone (Zone C in Fig. 6) is rather electrically homogeneous and relatively conductive (<200 Ω-m) with respect to the overlying electrical structure. Zone C could be related to the more plastic material of the asthenosphere.

The electrical homogeneity of the zone is disturbed below the south-western half of the profile with a region (Region 4 in Fig. 6) of intermediate electrical resistivities (200–800 Ω-m). This feature probably suggests a more gradual transition from the rigid material of the subducting African lithosphere to the more plastic material of the asthenosphere.

Below sites 6 and 5, the relatively resistive material of Region 1 (Zone B), seems to bent and continue vertically downwards within Zone C to a maximum depth of about 350 km. Although this feature seems to comply with the ideas of Ligdas et al. (1990), Ligdas and Main (1991), and Spakman et al. (1988, 1993), it is not adequately resolved and thus questioned in Fig. 6.

5. Conclusions

LMT data from 8 sites located along a 250 km NE–SW profile across the southern part of the Hellenic mainland were used to determine the deep geoelectric structure of HSZ. Application of both 1-D and 2-D modelling allowed the construction of corresponding electrical models.

A geoelectric model was adopted to account for the deep (40–400 km) electrical structure of HSZ. The proposed model was based on 2-D modelling attempts derived by using the method introduced by Mackie et al. (1988), since it had better maximum depth resolution of about 400 km and revealed structures not detected by the 1-D models. Inferences for the shallower (<40 km)

electrical structure were made by using the results of 1-D modelling.

The model structure related to the African and Euro-Asian lithosphere is relatively resistive (>800 Ω-m) and has an average thickness of 150–170 km. Although the bottom of the lithosphere is adequately resolved, the Wadati-Benioff zone that delineates the top of the subducting lithospheric slab is not identified by any electrical feature. The model structure, which is associated with the subducting part of the African lithosphere, penetrates a relatively conductive (<200 Ω-m) asthenosphere with a dip angle of 42°. The observed dip angle (42°) and the adequately resolved averaged penetration depth (250 km) of the subducting slab support the ideas of Doglioni et al. (1999) that HSZ is a NE-directed zone. However, the averaged penetration depth exceeds by 70 km that of the well-identified Wadati-Benioff zone.

Intermediate electrical resistivities (200–800 Ω-m) were attributed to the melting part of the lithosphere below the region of HVA and to a dipping zone below the south-western part of the profile at 170–220 km depths.

Acknowledgements

This paper is dedicated to the memory of Dr. Violet Rosemary Strachan Hutton as a last tribute to a generous personality, patient teacher, excellent supervisor and colleague, whose restless research mind was such and encouraged us to initiate the study of the deep electrical structure of HSZ.

This work was supported by the National Kapodistrian University of Athens (Greece), the General Secretariat for Research and Technology (Greece) and the British Council in Athens. We wish to thank Dr. B.A. Hobbs and Mr. G.J.K. Dawes for their valuable suggestions and help. We are grateful to the UK Natural Environment Research Council (NERC) Equipment Pool for the loan of three complete LMT data logging systems and particularly thankful to Mr. M.J. Valiant for providing technical advice and assistance on the use of the NERC LMT data logging systems. Also to Mr. I. Giannopoulos for assistance in the field.

References

Angelier, J., Lyberis, N., Le Pichon, X., Barrier, E., Huchon, P., 1982. The tectonic development of the Hellenic Arc and the Sea of Crete: a synthesis. Tectonophysics 86, 159–196.

Ansorge, J., Blundell, D., Mueller, S., 1992. Europe's lithosphere-seismic structure. In: Blundell, D., Freeman, R., Mueller, S. (Eds.), A Continent Revealed: The European Geotraverse. Cambridge University Press, Cambridge.

Calganile, G., D'Igneo, F., Farrugia, P., Panza, G.F., 1982. The lithosphere in the Central-Eastern Mediterranean area. Pure Appl. Geophys. 120, 389–406.

Chailas, S., Hipkin, R.G., Lagios, E., 1993. Isostatic studies in the Hellenides. Proc. 2nd Intern. Congr. Hellen. Geophys. Union, May 5–7, Florina, Greece, vol. 2, pp. 492–504.

Dawes, G.J.K., Lagios, E., 1991. A magnetotelluric survey of the Nisyros geothermal field (Greece). Geothermics 20, 225–235.

Deuss, A., Woodhouse, J.H., 2002. A systematic search for mantle discontinuities using SS-precursors. Geophys. Res. Lett. 29, 90-1–90-4.

Doglioni, C., Harabaglia, P., Merlini, S., Mongelli, F., Peccerillo, A., Piromallo, C., 1999. Orogens and slabs vs. their direction of subduction. Earth Sci. Rev. 45, 167–208.

Fytikas, M., Kolios, N.P., 1979. Preliminary heat flow map of Greece. In: Cermak, V., Rybach, L. (Eds.), Terrestrial Heat Flow in Europe. Springer-Verlag, p. 328.

Fytikas, M., Innocenti, F., Manetti, P., Mazzuoli, R., Peccerillo, A., Vilari, L., 1984. Tertiary to Quaternary evolution of volcanism in the Aegean region. Spec. Publ. - Geol. Soc. Lond. 17, 687–699.

Galanopoulos, A., 1963. On mapping of seismic activity in Greece. Ann. Geofis. 16, 37–100.

Galanopoulos, D., 1993. Preliminary magnetotelluric studies along the Hellenic Volcanic Arc: implications for the collision between the African plate and the "Aegea" microplate. Phys. Earth Planet Inter. 81, 139–153.

Galanopoulos, D., Hutton, V.R.S., Dawes, G.J.K., 1991. The Milos geothermal field: modelling and interpretation of electromagnetic induction studies. Phys. Earth Planet. Inter. 66, 76–91.

Galanopoulos, D., Lagios, E., Dawes, G.J.K., Hobbs, B.A., 1998. Geoelectric structure of Soussaki geothermal area (Greece) deduced from two dimensional magnetotelluric studies. J. Balk. Geophys. Soc. 1 (4), 60–74.

Groom, R.W., Bailey, R.C., 1989. Decomposition of magnetotelluric impedance tensors in the presence of local three-dimensional galvanic distortion. J. Geophys. Res. 94, 1913–1925.

Groom, R.W., Kurtz, R.D., Jones, A.G., Boerner, D.E., 1993. A quantitative methodology to extract regional magnetotelluric impedances and determine the dimension of the conductivity structure. Geophys. J. Int. 115, 1095–1118.

Gu, Y.L., Dziewonski, A.M., Ekstrom, G., 2001. Preferential detection of the Lechmann discontinuity beneath continents. Geophys. Res. Lett. 28, 4655–4658.

Hatzfeld, D., Pedotti, G., Hatzidimitriou, P., Panagiotopoulos, D., Scordilis, M., Drakopoulos, J., Makropoulos, K., Delibasis, N., Latousakis, I., Baskoutas, J., Frogneux, M., 1989. The Hellenic subduction beneath the Peloponnesus: first results of a micro-earthquake study. Earth Planet. Sci. Lett. 93, 283–291.

Hobbs, B.E., Ord, A., 1988. Plastic instabilities: implications for the origin of intermediate and deep focus earthquakes. J. Geophys. Res. 93, 10521–10540.

Hutton, V.R.S., Galanopoulos, D., Dawes, G.J.K., Pickup, G.E., 1989. A high resolution magnetotelluric survey of the Milos geothermal prospect. Geothermics 18 (4), 521–532.

Jones, A.G., 1983. On the equivalence of the "Niblett" and "Bostick" transformation in the magnetotelluric method. J. Geophys. 53, 72–73.

Jones, A.G., Groom, R.W., 1993. Strike angle determination from the magnetotelluric tensor in the presence of noise and local distortion: rotate at your peril! Geophys. J. Int. 113, 524–534.

Lagios, E., Galanopoulos, D., 1998. Geothermal prospection of Kimolos Island from magnetotelluric measurements. Proc. 8th

Intern. Congress, Geol. Soc. of Greece, Patra, May 27–29, vol. 32/4, pp. 255–265.

Lagios, E., Chailas, S., Hipkin, R.G., 1995. Gravity and isostatic anomaly maps of Greece produced. EOS, transactions. Am. Geophys. Union 76 (274 pp.).

Lagios, E., Galanopoulos, D., Hobbs, B.A., Dawes, G.J.K., 1998. Two dimensional magnetotelluric modelling of the Kos Island geothermal region (Greece). Tectonophysics 287, 157–172.

Le Pichon, X., Angelier, J., 1979. The hellenic arc and trench system: a key to the neotectonic evolution of the Eastern Mediterranean area. Tectonophysics 60, 1–42.

Ligdas, C.N., Main, I.G., 1991. On the resolving power of tomographic images in the Aegean area. Geophys. J. Int. 107, 197–203.

Ligdas, C.N., Main, I.G., Adams, R.D., 1990. 3-D structure of the lithosphere in the Aegean region. Geophys. J. Int. 102 (1), 219–229.

Mackie, R.L., Bennett, B.R., Madden, T.R., 1988. Long period magnetotelluric measurements near the Central California coast: a land locked view of the conductivity structure under the Pacific Ocean. Geophys. J. Int. 95, 181–194.

Mackie, R.L., 1996. Two Dimensional Inversion of Magnetotelluric Data, Software. Internet site: MTNET http://www.geophysics.dias.ie/mtnet/progs/progs.html.

Madden, T.R., Mackie, R.L., 1989. Three-dimensional magnetotelluric modelling and inversion. Proc. IEEE 77, 318–333.

Makris, J., 1985. Geophysics and geodynamic implications for the evolution of the Hellenides. In: Stanley, D., Wezel, F. (Eds.), Geological Evolution of the Mediterranean Basin. Springer, Berlin, pp. 231–248.

McKenzie, D.P., 1978. Active tectonics of the Alpine–Himalayan Belt: the Aegean sea and the surrounding regions. Geophys. J. R. Astron. Soc. 55, 217–254.

Meju, M.A., Hutton, V.R.S., 1992. Iterative most-squares inversion: application to magnetotelluric data. Geophys. J. Int. 108, 758–766.

Makropoulos, K.C., Burton, P.W., 1984. Greek tectonics and seismicity. Tectonophysics 106, 275–304.

Papadopoulos, G.A., Kondopoulou, D., Leventakis, G.A., Pavlides, S., 1986. Seismotectonics of the Aegean region. Tectonophysics 124, 67–84.

Papazachos, B.C., 1969. Phase velocities of Rayleigh waves in the south-eastern Europe and eastern Mediterranean sea. Pure Appl. Geophys. 75, 47–55.

Papazachos, B.C., 1973. Distribution of seismic foci in the Mediterranean and surrounding area and its tectonic implications. Geophys. J. R. Astron. Soc. 33, 421–430.

Papazachos, C.B., 1994. Structure of the crust and upper mantle in southeast Europe by inversion of seismic and gravimetric data. Doctorate Thesis. Aristotelian Univ. of Thessaloniki, Greece.

Papazachos, B.C., Karakostas, V.G., Papazachos, C.B., Scodilis, E.M., 2000. The geometry of the Wadatti-Benioff zone and lithospheric kinematics in the Hellenic Arc. Tectonophysics 319, 275–300.

Payo, G., 1967. Crustal structure of the Mediterranean Sea by surface waves: I. Group velocity. Bull. Seismol. Soc. Am. 57, 151–172.

Payo, G., 1969. Crustal structure of the Mediterranean Sea by surface waves: I. Phase velocity and travel time. Bull. Seismol. Soc. Am. 59, 23–42.

Sotiropoulos, P., Galanopoulos, D., Lagios, E., Dawes, G.J.K., 1996. An audio-magnetotelluric (AMT) survey on Santorini Volcano, Greece. Proc. 2nd Workshop on European Laboratory Volcanoes, May 2–4, Santorini, Greece (Publ. Europ. Comm. DGXII Environment and Climate Res. Progr.), pp. 281–295.

Spakman, W., Wortel, M.J.R., Vlaar, N.J., 1988. The Hellenic subduction zone: a tomographic image and its geodynamic implications. Geophys. Res. Lett. 15, 60–63.

Spakman, W., Van der Lee, R.D., Van der Hilst,, 1993. Travel time tomography of the European–Mediterranean mantle down to 1400 km. Phys. Earth Planet Inter. 79, 3–74.

Tsokas, G.N., Hansen, R.O., 1997. Study of the crustal thickness and the subducting lithosphere in Greece from gravity data. J. Geophys. Res. 102 (B9), 20585–20597.

Tzanis, A., Lagios, E., 1993. Magnetotelluric exploration of Sussaki geothermal prospect, Corinth Prefecture, Greece: the first results. Proc. 2nd Intern. Congr. Hellen. Geophys. Union, May 5–7, Florina, Greece, vol. 2, pp. 229–243.

Tzanis, A., Lagios, E., 1994. Magnetotelluric reconnaissance in Methana Peninsula Volcanic Complex (West Saronikos Gulf, Greece). Bull. Geol. Soc. Greece 30(5), 15–26.

Van der Meijde, M., Van der Lee, S., Giardini, D., 2003. Crustal structure beneath broad-band seismic stations in the Mediterranean region. Geophys. J. Int. 152, 729–739.

Wannamaker, P.E., Stodt, J.A., Rijo, L., 1986. Two-dimensional topographic responses in magnetotellurics modelled using finite elements. Geophysics 51, 2131–2144.

Wannamaker, P.E., Stodt, J.A., Rijo, L., 1987. A stable finite-element solution for two dimensional magnetotelluric modelling. Geophys. J. R. Astron. Soc. 88, 277–296.

Wortel, M.J.R., 1982. Seismicity and rheology of subducted slabs. Nature 296, 553–556.